CHAPTER 2: WAVEGUIDE ANALYSIS METHODS

2.1 Introduction

This chapter discusses the types of the waveguides and the behavior of light from the point of view of ray optics and electromagnetic theory, followed by a brief treatment on simulation techniques. Subsequently, the basic idea of the Finite Difference Method (FDM) will be elaborated further in Section 2.2 as will the effects of the boundary conditions. This is followed by a discussion on Beam Propagation Method (BPM) and how FDM is employed in BPM. The last section describes the Coupled Mode Theory (CMT) which is used to deal with coupling activities between two closely spaced waveguides.

2.2 Planar Waveguides

Planar waveguides are optical components that allow the confinement of light within certain boundaries by total internal reflection. Typically, there are three main types of basic waveguides structure commonly used in silica-on-silicon platform: ridge, rib, and buried waveguide as illustrated in Figure 2.1 [1]. In Figure 2.1, the waveguide core layer is shown in dark blue whereas the waveguide cladding is shaded in light blue.

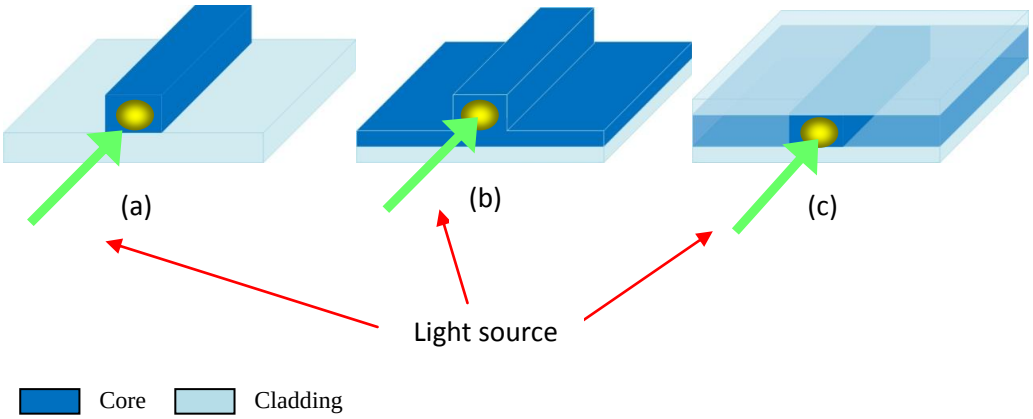

Figure 2.1: Three planar waveguide types: (a) ridge waveguide; (b) rib waveguide; and (c) buried waveguide.

The core layer has a higher refractive index than its surrounding cladding layer in order to keep the light (in the form of photon) well confined in the waveguide. It thus can be said that the cladding is treated as a protective layer to guide the light within the core with minimum losses and throughout this work, the buried waveguide is used. The mechanism of light guidance in the waveguide will be discussed in the next section.

2.2.1 Light Behavior from the Point of View of Ray Optics

Light behavior within a planar waveguide can be outlined and analyzed from the point of view of ray optics. Consider the planar waveguide illustrated in Figure 2.1(c), where core layer (dark blue) is enclosed or sandwiched by cladding layer (light blue). We assume n_1 to represent the refractive index value of the core layer and n_2 corresponding to the refractive index value of the cladding layer. In addition, we also assume that n_1 is higher than n_2. Thus, the propagation of light through the planar waveguide by Total Internal Reflection (TIR) can be intuitively understood by the use of the ray optics model.

As shown earlier, the flow of light within the waveguide is governed by Snell's Law. Snell's Law is used to describe the relationship that governs the light propagation, where incident angle θ_1 of light in a medium with index n_1 impinge on the boundary of a dissimilar medium with index n_2, resulting the light is refracted at angle of θ_2 as depicted in Figure 2.2 (a).

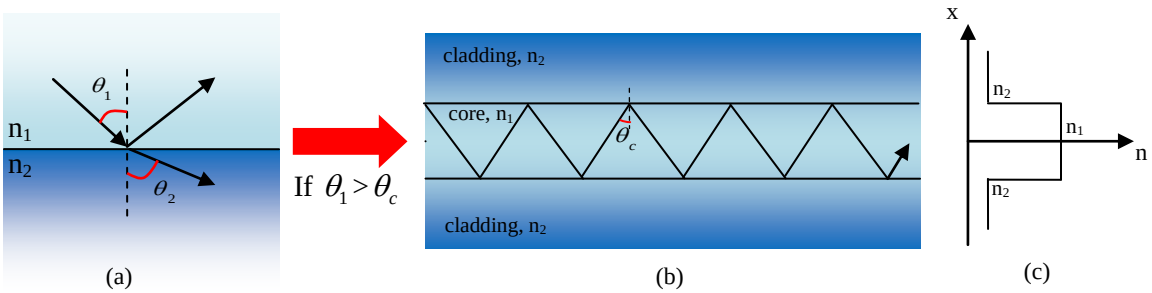

Figure 2.2: (a) Reflection and refraction at a plane interface, (b) propagation of light through optical waveguide by total internal reflection (TIR), (c) refractive index profile of the optical waveguide

The relationship that governs the light propagation that was derived from Snell's Law is shown below [2];

$$n_1 \sin\theta_1 = n_2 \sin\theta_2 \qquad (2.1)$$

θ is measured with respect to the normal of interface of two different medium. In order to confine light within the waveguide, n_1 has to be larger than n_2. Furthermore, if θ_2 becomes 90^o, a condition termed total internal reflection (TIR) occurs, where incident light impinging on the boundary is reflected back into same medium. The incident angle, θ_1 that allow for this situation is called the critical angle, θ_c. As such, equation 2.1 can be simplified to [2];

$$\theta_1 = \sin^{-1}(\frac{n_2}{n_1}) \tag{2.2}$$

It can be seen from Fig. 2.2(b), if incident angle θ_1 exceed θ_c, light will continue to be reflected at the interface and subsequently guided via TIR in the core layer [2]. The distribution of the refractive index which core layer has higher index value is illustrated in Fig. 2.2(c). It is found that a small portion of guided light is accumulated outside of core region. It is called evanescent field and this is very useful for energy transfer to another adjacent waveguide.

2.2.2 Light Behavior from the Point of View of Electromagnetic Theory

Although the ray optics approach can be utilized for qualitative description and basic understanding for light behavior within the waveguide, the technique lacks the information and ability to explain the relationship between the electric and magnetic field distribution. In many applications such as optical coupling, it is essential to know the distribution of optical field or intensity within the waveguide. Therefore it is necessary to include the more rigorous waveguide treatment based on Maxwell's equations.

The electromagnetic theory of light applied to the planar waveguide is described by Maxwell's equations [3-5]. We start the Maxwell's equations by assuming that the light is penetrating via a non-conductive dielectric (conductivity $\sigma = 0$), isotropic, non-magnetic (magnetic permeability $\mu = \mu_o$), and linear medium ($D = \varepsilon E$). Therefore, Maxwell's equations are reduced to [5]:

$$\nabla X\vec{E} = -\mu_o \frac{\partial \vec{H}}{\partial t} \tag{2.3}$$

$$\nabla X\vec{H} = \varepsilon_o n^2 \frac{\partial \vec{E}}{\partial t} \tag{2.4}$$

where $\vec{E}$ and $\vec{H}$ are the electric and magnetic fields respectively, μ_o is the free space permeability, ε_o is the permittivity of the free space and *n* is the refractive index of the light propagation medium. Under the conditions mentioned above, it is noted that div E and div H are equal to zero.

For an optically inhomogeneous medium with the refractive index changes only in the transverse direction, $n = n(r)$ and using Maxwell's equations (2.3) and (2.4), we obtain the following wave equations for $\vec{E}$ and $\vec{H}$ [5]:

$$\nabla^2\vec{E} + \nabla(\frac{1}{n^2}\nabla n^2\vec{E}) - \varepsilon_o\mu_o n^2 \frac{\partial^2\vec{E}}{\partial t^2} = 0 \tag{2.5}$$

$$\nabla^2\vec{H} + \frac{1}{n^2}\nabla n^2 X(\nabla X\vec{H}) - \varepsilon_o\mu_o n^2 \frac{\partial^2\vec{H}}{\partial t^2} = 0 \tag{2.6}$$

The above equations indicate that the Cartesian components of the electric field vector E_x, E_y and E_z and magnetic field vector H_x, H_y and H_z are coupled in an inhomogeneous medium. In this regard, a scalar wave equation for each component cannot be established as in the case of a homogeneous medium. However, the adequate solution to the inhomogeneous wave equations (2.5) and (2.6) for monochromatic wave is described by the form [5]:

$$\vec{E}(r,t) = E(x,y)e^{i(\omega t - \beta z)} \tag{2.7}$$

$$\vec{H}(r,t) = H(x,y)e^{i(\omega t - \beta z)} \tag{2.8}$$

where β is the propagation constant and ω being the angular frequency of the wave. These two expressions indicate the electromagnetic field for a propagating mode. By applying the solution for planar waveguide given in equations (2.7) and (2.8) to Maxwell's equations in equations (2.3) and (2.4), and taking their x, y and z components as shown in Figure 2.3, we obtain the following expressions [5]:

$$\frac{\partial E_z}{\partial y} + j\beta E_y = -j\omega_o \mu H_x \tag{2.9}$$

$$\frac{\partial E_y}{\partial x} - \frac{\partial E_x}{\partial y} = -j\omega_o \mu H_z \tag{2.10}$$

$$j\beta H_x + \frac{\partial H_z}{\partial x} = -j\omega_o \varepsilon n^2 E_y \tag{2.11}$$

$$\frac{\partial H_z}{\partial y} + j\beta H_y = j\omega_o \varepsilon n^2 E_x \tag{2.12}$$

$$\frac{\partial H_y}{\partial x} - \frac{\partial H_x}{\partial y} = j\omega_o \varepsilon n^2 E_z \tag{2.13}$$

$$j\beta E_x + \frac{\partial E_z}{\partial x} = j\omega_o \mu H_y \tag{2.14}$$

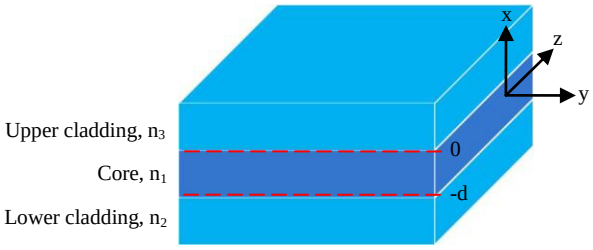

Figure 2.3: The basic structure of the slab waveguide where the core layer is sandwiched between upper cladding and lower cladding

In the case of wave guiding confined to one direction (one dimension confinement), the confinement is assumed to be in x-direction within the core layer. In addition, the upper and lower cladding layers are respectively assumed to be infinity. Furthermore, the light is assumed to propagate in z-direction and the waveguide is also assumed no dependence in y-direction. Therefore the electric and magnetic fields in the planar waveguide show independence on y-direction and by setting $\frac{\partial \vec{E}}{\partial y} = 0$ and $\frac{\partial \vec{H}}{\partial y} = 0$ equations (2.9) to (2.14) can be simplified to [5]:

$$\beta E_y = -\omega_o \mu H_x \tag{2.15}$$

$$\frac{\partial E_y}{\partial x} = -j\omega_o \mu H_z \tag{2.16}$$

$$j\beta H_x + \frac{\partial H_z}{\partial x} = -j\omega_o \varepsilon n^2(x) E_y \tag{2.17}$$

$$\beta H_y = -\omega_o \varepsilon n^2(x) E_x \tag{2.18}$$

$$\frac{\partial H_y}{\partial x} = j\omega_o \varepsilon n^2(x) E_z \tag{2.19}$$

$$j\beta E_x + \frac{\partial E_z}{\partial x} = j\omega_o \mu H_y \tag{2.20}$$

The first three equations only involve E_y , H_x and H_z and the last three expressions involve E_x, E_z and H_y. The first set of equations, equations (2.15) to (2.17) corresponds to the TE (transverse electric) modes as TE modes only contain the transverse component (E_y) with respect to the direction of propagation z, thus $E_z = 0$. Meanwhile the second set of equations are denoted as TM (transverse magnetic) modes which having the non-vanishing value of E_x, E_z and H_y. Similarly, the magnetic fields have only a transverse component (H_y) and no magnetic field along the z direction, hence $H_z = 0$.

As discussed earlier, the propagation of light within a planar waveguide may be described in terms of TE modes and TM modes. We first consider the TE modes by substituting H_x and H_z components from equations (2.15) and (2.16) into equation (2.17) to obtain the TE wave equation for E_y as [5]

$$\frac{\partial^2 E_y}{dx^2} + [k_o^2 n^2(x) - \beta^2]E_y = 0 \qquad (2.21)$$

where the free space wave number is given by, $k_o = \omega_o \sqrt{\varepsilon_o \mu_o}$.

The analysis so far is valid for an arbitrary x-dependent profile. Referring back to Figure 2.3, the core layer which has a refractive index value, n_1 is sandwiched between two cladding layers which have refractive index values n_2 and n_3. They are separated by planar boundaries perpendicular to the x-axis. In this case, z is the propagation axis for the light beam. In order to confine the light beam to within the waveguide, we assume $n_1 > n_2 > n_3$. The plane

$x = 0$ corresponds to the upper cladding-core boundary and the core-lower cladding boundary is located at $x = -d$. Thus the core thickness is d. The specific index profile of planar waveguide structures as depicted in Figure. 2.3 is utilized and given as below:

$$n(x) = \begin{cases} n_1; & -d < x < 0 \\ n_2; & x \le -d \\ n_3; & x \ge 0 \end{cases} \tag{2.22}$$

The mode that is mainly confined within the core layer is denoted as guided modes and its power decay exponentially in the cladding. To fulfill boundary condition at $-d < x < 0$, the propagation constant β associated with a particular mode must have:

$$k_o n_2 < \beta < k_o n_1 \tag{2.23}$$

In term of the refractive index, the effective index N of guided mode must be located between n_1 and n_2:

$$n_2 < N < n_1 \tag{2.24}$$

where $N = \frac{\beta}{k_o}$. By imposing suitable boundary conditions, the wave equation from (2.21) can be written as [5]:

$$\frac{\partial^2 E_y}{dx^2} + \gamma_1^2 E_y = 0 \quad x \geq 0 \text{ (upper cladding)} \tag{2.25}$$

$$\frac{\partial^2 E_y}{dx^2} + \gamma_2^2 E_y = 0 \quad x \leq -d \text{ (lower cladding)} \tag{2.26}$$

$$\frac{\partial^2 E_y}{dx^2} + \kappa^2 E_y = 0 \quad -d < x < 0 \text{ (cover)} \tag{2.27}$$

where the two parameters γ and κ are shown follows:

$$\gamma_1^2 = \beta^2 - k_o^2 n_3^2 \tag{2.28}$$

$$\kappa^2 = k_o^2 n_1^2 - \beta^2 \tag{2.29}$$

$$\gamma_2^2 = \beta^2 - k_o^2 n_2^2 \tag{2.30}$$

The solution of the electric field in the upper cladding, core and lower cladding from equation (2.25) - (2.27) can be presented as [5]:

$$E_y = \begin{cases} Ae^{-\gamma_1 x} & x \geq 0 \\ Be^{i\kappa x} + Ce^{-i\kappa x} & -d < x < 0 \\ De^{\gamma_2 x} & x \leq -d \end{cases} \tag{2.31}$$

where A, B, C and D are constant. Applying the continuity of E_y and $\frac{dE_y}{dx}$ at the boundaries $x = 0$ and $x = -d$ yields the four equations that related to constants A, B, C and D and propagation constant β [5]:

$$B + C = A \tag{2.32}$$

$$Be^{-i\kappa d} + Ce^{i\kappa d} = De^{-i\gamma_1 d} \tag{2.33}$$

$$i\kappa B - i\kappa C = -\gamma_1 A \tag{2.34}$$

$$i\kappa Be^{-i\kappa d} - i\kappa Ce^{i\kappa d} = \gamma_2 De^{-\gamma_2 d} \tag{2.35}$$

By solving equations (2.32) to (2.35), the following equation is acquired [5]:

$$\tan \kappa d = \frac{\left(\frac{\gamma_1}{\kappa}\right) + \left(\frac{\gamma_2}{\kappa}\right)}{1 - \left(\frac{\gamma_1}{\kappa}\right)\left(\frac{\gamma_2}{\kappa}\right)} \tag{2.36}$$

The relation above can be considered as the dispersion relation for the asymmetric step index planar waveguide and is a transcendental equation which will determine the values of propagation constant. For the case of symmetric step index planar waveguide ($n_2 = n_3$), the transcendental equation is reduced to:

$$\tan \kappa d = \frac{2\left(\frac{\gamma_1}{\kappa}\right)}{1 - \left(\frac{\gamma_1}{\kappa}\right)^2} \tag{2.37}$$

where $\gamma_1 = \gamma_2$. The following descriptions only take account of asymmetric step index planar waveguide. It is simple to modify the asymmetric expressions to symmetric expression. In order to transcendental equation in equation (2.36) can be universalized for any asymmetric step index waveguide, it is convenient to introduce a set of normalized parameters:

$$b = \frac{(N^2 - n_2^2)}{\left(n_1^2 - n_2^2\right)}; \quad \text{Normalized mode index,} \tag{2.38}$$

$$V = k_o d (n_1^2 - n_2^2)^{\frac{1}{2}}; \quad \text{Normalized core thickness/V-number,} \tag{2.39}$$

$$\text{and} \quad a = \frac{(n_2^2 - n_3^2)}{\left(n_1^2 - n_2^2\right)}; \quad \text{Asymmetry measure.} \tag{2.40}$$

The effective index N corresponding to a confined mode is in the range of $n_2 < N < n_1$ whereas the normalized mode index b is bounded between 0 and 1. As deduced from equation (2.39), the normalized core thickness V or V-number is proportional to the thickness of core layer d and inversely proportional to wavelength λ. The V-number includes all the waveguide parameters that will determine the guidance behavior of the waveguide. On the other hand, the asymmetry measured at a is zero in the case of symmetric waveguide, thus $n_2 = n_3$.

By rearranging the transcendental equation, it can be rewritten as the function of propagation constant β and in terms of the normalized parameters [5]:

$$\tan\left[V\sqrt{1-b}\right] = \frac{\sqrt{\frac{b}{1-b}} + \sqrt{\frac{b+a}{1-b}}}{1 - \frac{\sqrt{b(b+a)}}{(1-b)}} \tag{2.41}$$

The electric field in the three different regions can be determined after the propagation constant β is obtained numerically from equation (2.41):

$$E_y = \begin{cases} Ae^{-\gamma_1 x} & x \geq 0 \\ A(\cos \kappa x - \frac{\gamma_1}{\kappa} \sin \kappa x) & -d < x < 0 \\ A(\cos \kappa d + \frac{\gamma_1}{\kappa} \sin \kappa d) e^{\gamma_2 (x+d)} & x \leq -d \end{cases} \tag{2.42}$$

Based on expressions above, the electrical fields decrease exponentially in upper and lower cladding layers whilst the electrical fields vary sinusoidal in the core layer. The solution for E_y is completely validated except the constant A. It is related to the energy carried by the mode.

Following the same procedure in determining E_y, the magnetic field component H_y of a particular guided mode can be obtained. The wave equation for TM propagation mode is identical to that obtained in TE, with the exception that the magnetic field function has been established. TM wave equation for H_y is given as below:

$$\frac{\partial^2 H_y}{dx^2} + [k_o^2 n^2(x) - \beta^2] H_y = 0 \tag{2.43}$$

The transcendental equation for TM waveguide is obtained in terms of normalized parameters [5]:

$$\tan\left[V\sqrt{1-b}\right] = \frac{\frac{1}{\gamma_a}\sqrt{\frac{b}{1-b}} + \frac{1}{\gamma_b}\sqrt{\frac{b+a}{1-b}}}{1 - \frac{1}{\gamma_a \gamma_b}\frac{\sqrt{b(b+a)}}{(1-b)}} \tag{2.44}$$

For the sake of simplicity, the γ_a and γ_b are respectively defined as $\gamma_a = \left(\frac{n_2}{n_1}\right)^2$ and $\gamma_b = \left(\frac{n_3}{n_1}\right)^2 = \gamma_a - a(1-\gamma_b)$. The solutions for the magnetic field are [ref]:

$$E_y = \begin{cases} Ae^{-\gamma_1 x} & x \geq 0 \\ A(\cos \kappa x - \frac{n_1^2}{n_3^2}\frac{\gamma_1}{\kappa}\sin \kappa x) & -d < x < 0 \\ A(\cos \kappa d + \frac{n_1^2}{n_3^2}\frac{\gamma_1}{\kappa}\sin \kappa d)e^{\gamma_2(x+d)} & x \leq -d \end{cases} \quad (2.45)$$

The objective of the above discussion is to provide both qualitative and quantitative picture about the guidance behavior of the waveguide. Nevertheless, the theoretical treatment above is only restricted to the slab waveguide structure as depicted in Figure 2.3. In the latter section, we will discuss the methods which can be implemented for the guidance in channel waveguide. There are numerous methods are available including effective index method [6, 7], Marcatili's method [8] and the FDM [9]. The first two techniques are considered as analytical method and they will not be utilized throughout the work. It is found that the analytical method is accurate than the numerical method. However the FDM as a numerical method is employ in this work and will be elucidated at next section.

2.3 The Finite Difference Method (FDM)

As discussed earlier, the electromagnetic fields propagating along the waveguide are composed of guided modes, also can be addressed as eigenmodes, which are dominated by transverse electric and magnetic field components with their corresponding propagation constants. The behavior of these electromagnetic fields can be analyzed and derived from the Maxwell's equations. The analytical solution is acquired by solving the Maxwell's equations. Nevertheless, this is only for simple waveguide geometries such as slab waveguides. For this reason, solving electromagnetic problems for practical waveguide geometries requires the use of numerical methods. Numerical methods are based on the approximation to the exact solution and the standard that minimizes the error between the two. In the literature, there are several numerical methods available such as FDM [10], Finite Element Method (FEM) [11] and Method of Lines (MoL) [12] that can be used to solve the eigenmode. Throughout this work, the FDM is employed to analyze the eigenmode characteristics of an optical waveguide owing to its good numerical efficiency and accuracy.

In the FDM, the cross-section of the waveguide is made discrete with a rectangular grid of points which might be of identical or variable spacing as illustrated in Figure 2.4. In each of the subdivisions, a two-dimensional wave equation is replaced with appropriate Finite Difference relationship which is derived from a five-point Taylor series formula [10]. Each grid of point is assigned to an arbitrary electric field value. Due to the subdivisions being rectangular, thus the FDM is appropriate for rectangular waveguide structure. As shown in Figure 2.4, by defining ϕ to be electric field component to be calculated, the relationships are shown as below:

$$\frac{\partial^2\phi}{dx^2} = \frac{\phi(m+1,n) - 2\phi(m,n) + \phi(m-1,n)}{\Delta x^2}, \text{ and} \tag{2.46}$$

$$\frac{\partial^2\phi}{dy^2} = \frac{\phi(m,n+1) - 2\phi(m,n) + \phi(m,n-1)}{\Delta y^2} \tag{2.47}$$

where Δx^2 and Δy^2 are spacing between two grid of points in x and y direction respectively.

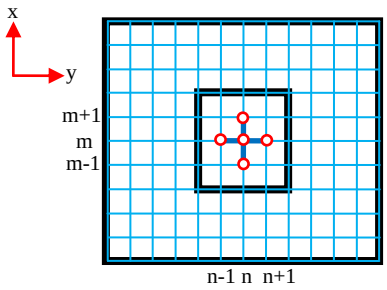

Figure 2.4: The cross-section of the waveguide is made discrete with a rectangular grid of points which have identical spacing.

There is a variety of boundary conditions that can be imposed at the edge of the analysis window such as Dirichlet, Neumann [13] and Transparent Boundary Condition (TBC) [14, 15]. The first and second boundary conditions for the calculation window are categorized as fixed boundary condition. This means that the field (electric or magnetic fields) is required to be set to zero at the boundary of the analysis window. It is a good approximation if there is a large index discontinuity at the edge. Nevertheless, it effectively reflects back the radiation to the analysis domain. To eliminate the back reflections or incoming fluxes into the analysis window, the TBC is applied. It effectively allows radiation to pass through the boundary freely and leave the analysis domain without appreciable reflection. In this way, the unwanted interference in the solution region (core layer) can be prevented [15].

2.4 Finite Difference Beam Propagation Method

As discussed in the previous section, FDM shows an excellent way to solve the waveguide eigenmode. Nevertheless it could not be utilized in solving the propagation characteristic in integrated optics and fiber optics. Figure 2.5 shows the 3-Dimensional Finite Difference as a plane rather than a ling along the z-axis.

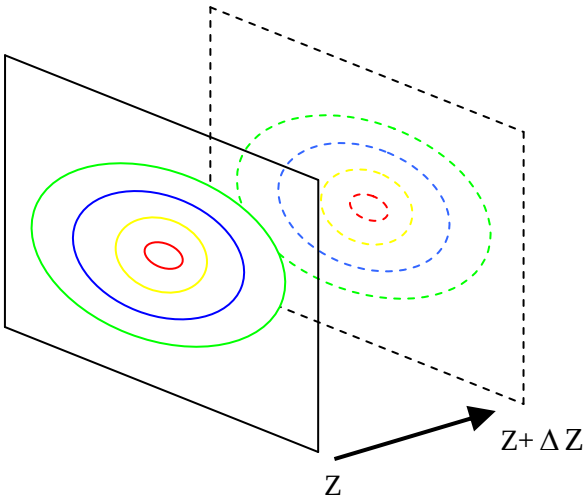

Figure 2.5: The 3D FD algorithm propagates a plane rather than a line along the z-propagation direction.

The BPM is a widely used and indispensable numerical technique in today's modeling and simulation of evolution of electromagnetic fields in arbitrary inhomogeneous medium. BPM is eligible to apply in complex geometries and automatically consider both guided and radiation modes [10]. There are several numerical methods that can be employed in BPM including Fast Fourier Transform Method (FFT) [16], (FEM [17] and FDM [18]. In this project, the Finite Difference Beam Propagation Method (FD-BPM) is employed to investigate light propagation in the silica based pump/signal MUX.

2.4.1 Beam Propagation Method

Simulation and design works involve approximation [19]. In short, the BPM employs the FDM to solve the well-known parabolic or paraxial approximation of Helmholtz equation [20]. BPM was proposed by Fleck et al. (1976) [21] for solving the scalar Helmholtz equation. However BPM only started to be used in analyzing and designing integrated optic devices in 1983 by Feit et al. [22]. Although BPM is a solution for paraxial forward propagating wave but it can be expanded to include effects such as wide angle propagation via Padé approximation, polarization effect and bi-direction propagation.

As discussed earlier, BPM is a particular approach for approximating the exact wave equation for monochromatic waves and it can be solved numerically by FDM [23]. In this section, the main features of BPM and its boundary condition will be summarized by formulating the problem under restriction of scalar field (neglect polarization effect) and paraxiality (propagation is restricted to a narrow ranges of angles) [20]. The three-dimensional scalar wave equation can be written in the form of Helmholtz equation for monochromatic wave as [4]:

$$\frac{\partial^2 E}{dx^2} + \frac{\partial^2 E}{dy^2} + \frac{\partial^2 E}{dz^2} + k^2 n^2(x, y, z)E = 0 \qquad (2.48)$$

The slowly varying envelope approximation is used to approximate the electric field $E(x, y, z)$ in the +z direction. In this approximation, $E(x, y, z)$ is separated into two parts: the axially slowly varying envelope term of $\phi(x, y, z)$ and the rapidly varying term of $\exp(-jkn_o z)$. Then $E(x, y, z)$ can be expressed as:

$$E(x,y,z) = \phi(x,y,z)\exp(-jkn_o z) \tag{2.49}$$

where the notation of n_o is a refractive index in the cladding. Substituting the equation (2.49) into (2.48), we get

$$\nabla^2\phi - j2kn_o\frac{\partial\phi}{\partial z} + k^2(n^2 - n_o^2)\phi = 0 \tag{2.50}$$

where ∇^2 is Laplacian equation and is expressed as

$$\nabla^2 = \frac{\partial^2}{\partial x^2} + \frac{\partial^2}{\partial y^2} + \frac{\partial^2}{\partial z^2} \tag{2.51}$$

By assuming the weakly guiding condition ($(n^2 - n_o^2) \cong 2n_o(n - n_o)$), the equation (2.50) can be rewritten as:

$$\frac{\partial\phi}{\partial z} = -j\frac{1}{2kn_o}\nabla^2\phi - jk(n - n_o)\phi \tag{2.52}$$

The above is the wide-angle BPM equation. However, when $\frac{\partial^2\phi}{\partial z^2} = 0$, the equation (2.52) is reduced to:

$$\frac{\partial\phi}{\partial z} = -j\frac{1}{2kn_o}\left(\frac{\partial^2\phi}{\partial x^2} + \frac{\partial^2\phi}{\partial y^2}\right) - jk(n - n_o)\phi \tag{2.53}$$

This is the para-axial 3D BPM equation. 2D BPM equation is obtained by omitting the y-direction dependency.

2.4.2 Beam Propagation Method Based On Finite Difference

For simplicity, BPM analysis based on finite difference in this section will be developed in 2D scalar Helmholtz scalar wave equation which is expressed as:

$$\frac{\partial \phi}{\partial z} = -j\frac{1}{2kn_o}\frac{\partial^2 \phi}{\partial x^2} - \alpha(x,z)\phi - j\frac{k}{2n_o}[n^2(x,z) - n_o^2]\phi \tag{2.54}$$

In equation (2.54), $(n^2 - n_o^2)$ is not approximated as $2n_o(n-n_o)$ [4]. Hence, equation (2.54) can be used in both weakly guiding and strong guiding conditions. In general, a differential equation of the form:

$$\frac{\partial \phi}{\partial z} = A(x,z)\frac{\partial^2 \phi}{\partial x^2} - B(x,z)\phi \tag{2.55}$$

which can then be can be approximated by FDM as:

$$\frac{\partial \phi}{\partial z} \rightarrow \frac{\phi_i^{m+1} - \phi_i^m}{\Delta z}, \tag{2.56}$$

$$A(x,z)\frac{\partial^2 \phi}{\partial x^2} \rightarrow \frac{1}{2}A_i^{m+1/2}\left\{\frac{\phi_{i-1}^m - 2\phi_i^m + \phi_{i+1}^m}{(\Delta x)^2} + \frac{\phi_{i-1}^{m+1} - 2\phi_i^{m+1} + \phi_{i+1}^{m+1}}{(\Delta x)^2}\right\}, \text{ and} \tag{2.57}$$

$$B(x,z)\phi \rightarrow \frac{1}{2} B_i^{m=1/2}(\phi_i^{m+1} + \phi_i^m) \tag{2.58}$$

where Δx and Δz imply the compute step in the x- and z-axis respectively. Meanwhile subscript i and superscript m are the respective grid point along the x- and z-axis. Comparing equation (2.54) and (2.55), we get:

$$A = -j\frac{1}{2kn_o} \tag{2.59}$$

$$B = -\alpha(x,z) - j\frac{k}{2n_o}[n^2(x,z) - n_o^2] \tag{2.60}$$

Substituting equation (2.56)-(2.60) into equation (2.54), we acquire the following equations:

$$-\phi_{i-1}^{m+1} + s_i^m \phi_i^{m+1} - \phi_{i+1}^{m+1} = \phi_{i-1}^m + q_i^m \phi_i^m + \phi_{i+1}^m \equiv d_i^m, \tag{2.61}$$

$$s_i^m = 2 - k^2(\Delta x)^2[(n_i^{m+1/2})^2 - n_o^2] + j\frac{4kn_o(\Delta x)^2}{\Delta z} + j2kn_o(\Delta x)^2\alpha_i^{m+1/2}, \text{ and} \tag{2.62}$$

$$q_i^m = -2 + k^2(\Delta x)^2[(n_i^{m+1/2})^2 - n_o^2] + j\frac{4kn_o(\Delta x)^2}{\Delta z} - j2kn_o(\Delta x)^2\alpha_i^{m+1/2} \tag{2.63}$$

Therefore when the initial electric field $\phi_i^{m=0}$ is given at z=0, the electric field ϕ_i^m at the next propagation step, $z=z_m$ can be obtained by computing the equation (2.61). The FD-BPM based on 3D Helmholtz wave equation can be found in the following literature [4]. The Transparent Boundary Condition (TBC) [14] is imposed to FDBPM instead of Dirichlet condition ($\phi = 0$) and Neumann

condition ($\frac{\partial \phi}{\partial x} = 0$) to reduce reflection from incoming radiation field. TBC serve as a boundary when the radiation reach the edge of simulation window, it disappears into the boundary without any reflection.

2.5 Physics of Coupled Waveguide Device

An analysis for the coupling is a critical part to the design of a wide range of coupled waveguide devices including directional coupler, Mach-Zender interferometer, bragg grating, ring resonator and modulator. Hence, coupled mode theory is employed to calculate the coupling along the interaction length and outputs at various wavelengths.

2.5.1 Coupling of Light between Waveguide

The coupling activities are taking place between two adjacent waveguides owing to the waveguide mode evanescent fields overlapping. When the lights propagate in a waveguide, small portions of mode or evanescent field propagate into cladding region as illustrated in Figure 2.6.

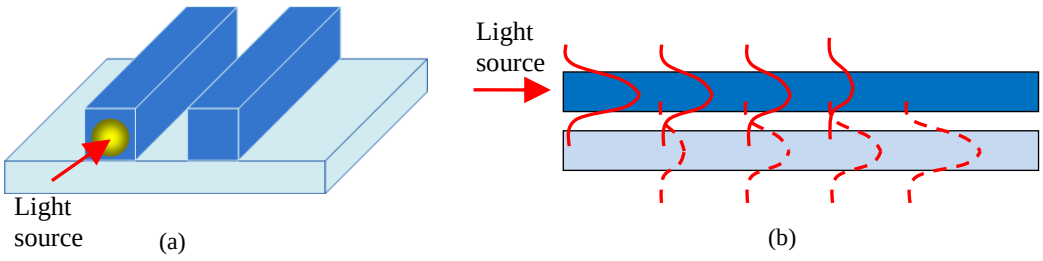

Figure 2.6: (a) the basic structure of two adjacent waveguide (b) when the lights launch into an input and propagate down a waveguide, small portions of evanescent field propagate into cladding region.

The intensity of the evanescent field decay exponentially with escalating the distance into the cladding region [24]. The coupling activities occur between waveguides only if both waveguides are placed sufficiently close to each other. The coupling activities are due to the significant overlapping of evanescent field between one waveguide to the adjacent one [25]. In this condition, the light energy will be transferred completely from one waveguide to the other in a periodic manner along the transmission direction [26]. The desired fraction of light energy can be obtained at a specific length.

2.5.2 Coupled Mode Theory

Generally, the CMT is a method that can be utilized for dealing with the mutual lightwave interaction between two propagation modes [4]. The behavior of two modes having mutual coupling is described by the Maxwell's equations. Nevertheless a basic understanding of mutual coupling can be acquired from coupling mode equations [4]:

$$\frac{dA(z)}{dz} = -i\kappa B(z)e^{-i(\beta_b-\beta_a)z}, \text{ and} \tag{2.64}$$

$$\frac{dB(z)}{dz} = -i\kappa A(z)e^{i(\beta_b-\beta_a)z} \tag{2.65}$$

where $A(z)$ and $B(z)$ are field amplitudes as a function of propagation in z-direction in the respective waveguide. β_a and β_b are the propagation constant in each waveguide whereas κ is a coupling coefficient. In this case, we assume two guided modes propagating in the same direction (+z direction), thus

$\beta_a > 0$ and $\beta_b > 0$. Equations (2.64) and (2.65) indicate the inter-relationship of the respective field amplitudes in each waveguide. With the initial condition $A(0) = 1$ and $B(0) = 0$ which correspond to the one optical input, the solution to equations (2.63) and (2.64) can be obtained [4]:

$$A(z) = e^{-i\Delta z}\left[\cos\gamma z + i\frac{\Delta}{\gamma}\sin\gamma z\right] \tag{2.66}$$

$$B(z) = -e^{i\Delta z}\frac{i\kappa}{\gamma}\sin\gamma z \tag{2.67}$$

where $2\Delta \equiv \beta_b - \beta_a$, corresponding to degree of synchronism between the mode a and b. The parameter γ defined as $\gamma = \pm\left(\kappa^2 + \Delta^2\right)^{1/2}$. From the solution above, it can be seen that the propagation mode (energy) will transmit back and forth between two waveguides in a periodic manner. The complex number indicates the phase change occurring each time the mode is transferred to another waveguide. It is also apparent seen that the coupling coefficient κ plays an important role in coupling activities.

The power flow in waveguide described by $|A(z)|^2$ and $|B(z)|^2$ and can be expressed as:

$$\frac{|A(z)|^2}{|A(0)|^2} = 1 - F\sin^2\gamma z \tag{2.68}$$

$$\frac{|B(z)|^2}{|A(0)|^2} = F\sin^2\gamma z \tag{2.69}$$

where $F \equiv \left(\frac{\kappa}{\gamma}\right)^2 = \frac{1}{1+(\Delta/\kappa)^2}$ .The minimum distance to achieve a complete coupling process (maximum power transfer) is defined as the coupling length, L_c given by [4]:

$$L_c = \frac{m\pi}{2\kappa}, \text{ for integer values of m} \tag{2.70}$$

where κ is the coupling coefficient of the two waveguides. The coupling coefficient κ is a parameter used to measure the degree of overlap that occurs between the evanescent fields of each waveguide [4]. Based on mode interference phenomena, the coupling coefficient κ can be acquired by analyzing both even and odd modes in the waveguides. Therefore, according to the mode interference phenomena, the minimum distance required for the complete transfer of light energy from one input waveguide to another waveguide is:

$$L_c = \frac{\pi}{\beta_e - \beta_o} \tag{2.71}$$

where β_e and β_o are the propagation constant for even and odd modes, respectively. Hence the coupling coefficient obtained from equation (2.69) and (2.70) is given by [4]:

$$\kappa = \frac{\beta_e - \beta_o}{2} \tag{2.72}$$

Therefore, the CMT is a crucial and important theory for designing and optimizing passive optical planar waveguide device in this work.

2.6 Summary

In this chapter, waveguide analysis methods were described. Initially, the chapter gave a brief description of planar waveguide structure. The buried waveguide is utilized throughout the work. The light behavior was elaborated in terms of ray optics and electromagnetic theory. The ray optics approach only can be utilized for qualitative description. Therefore, electromagnetic theory is applied to explain the relationship between electric and magnetic field distribution. Some derivations work on obtaining EM field distribution has been carried out. However the theoretical approaches above is only used for slab waveguide and there is necessary to use numerical method solver such as Finite Difference Method to solve the wave equation for buried waveguide. Finite Difference Beam Propagation Method (FDBPM) was employed to investigate light propagation in the buried waveguide. Transparent Boundary Condition (TBC) was imposed to FDBPM to reduce reflection from incoming light. Finally, the Coupled Mode Theory (CMT) was introduced and discussed. Coupling length, L_c give a rough indication for designing and optimizing the pump/signal multiplexer in the next chapter.

2.7 References

[1] Keigo Iizuka, "Element of Photonics Volume II," John Wiley & Son Inc., 2002.

[2] H. Kogeinik, "Theory of Optical Waveguides,"Guided-Wave Optoelectronics, 1990.

[3] A. Ghatak and K. Thyagarajan, "Introduction to Fiber Optics, 2nd ed," Cambridge Press, USA, 2000.

[4] K. Okamoto, "Fundamentals of optical waveguide," Academic Press, USA, 2006.

[5] Gin´es Lifante, "Integrated Photonics: Fundamentals," John Wiley & Son Ltd, 2002.

[6] G. B. Hocker and W. K. Burns, "Mode dispersion in diffused channel waveguides by the effective index method," Applied Optics **16**, 113-118 (1977).

[7] Qian Wang, Gerald Farrell, Thomas Freir," Effective index method for planar lightwave circuits containing directional couplers, Optics Communications," Optics Communications **259**(1), 133-136 (2006).

[8] E. A. J. Marcatili, "Dielectric rectangular waveguide and directional coupler for integrated optics," Bell Systems Tech. Journal **48**, 2071-2102 (1969).

[9] MS Stern, "Finite difference analysis of planar optical waveguides," Methods for modeling and simulation of guided-wave optoelectronic devices: modes and couplings PIER 10, EMW Publishing (1995).

[10] R. Scarmozzino, A. Gopinath, R. Pregla, S. Helfert, "Numerical Techniques for Modeling Guide-Wave Photonics Devices," IEEE Journal of Selected Topics in Quantum Electronics **6**(1), 150-162 2000.

[11] J. Jin, "The Finite Element Method in Electromagnetics, 2nd ed.," New York: John Wiley & Sons, 2002.

[12] J. S. Gu, P.A. Besse, and H. Melchior, "Method of lines for the analysis of the propagation characteristics of curved optical rib waveguides," IEEE J. Quantum Electron. **27**(3), 531-537 1991.

[13] Kenji Kawano and Tsutomu Kitoh, "Introduction to optical waveguide analysis: Solving Maxwell's equation and the Schrodinger equation," John Wiley & Son, 2001.

[14] H. J. W. M. Hoekstra, "Theory and Numerical Strategies of BPMs: On beam propagation methods for modelling," Optical and Quantum Electronics **29**, 157-171 1997.

[15] F. Fogli, G. Bellanca, P. Bassi, "TBC and PML conditions for 2D and 3D BPM: a comparison," Optical and Quantum Electronics **30**, 443-456 (1998)

[16] P. Pantelakis, and E. E. Kriezis, "Modified two-dimensional fast Fourier transform beam propagation method for media with random variations of refractive index," J.Opt.Soc.Am.A, **13**(9), 1884-1890 (1996).

[17] B. A. M. Rahman and J. B. Davies, "Finite element analysis of optical and microwave problems," IEEE Trans. Microwave Theory Tech **32**, 20-28 (1983).

[18] J. Yamauchi, J. Shibayama, O. Saito, O. Uchiyama, and H. Nakano, "Improved Finite-Difference Beam-Propagation Method Based on the Generalized Douglas Scheme and Its Application to Semivectorial Analysis," J.Lightwave Technol. **14**(10), 2401-2406 (1996).

[19] Trevor M. Benson, E. V. Bekker, Ana Vukovic, and Phillip Sewell, "Challenges for integrated optics design and simulation," Proc. SPIE **6796**, 67963C (2007).

[20] Robert Scarmozzino, “Simulation tools for devices, systems, and networks,” Optical Fiber Telecommunications V B: Systems and Networks, 803-863, 2008.

[21] S.T. Chu, W.P. Huang and S.K. Chaudhuri, “Simulation and analysis of waveguide based optical integrated circuits,” Computer Physics Communications **68**, 451-484 (1991).

[22] G.L. Yip, “Design Methodology for Guided-Wave Photonic Devices,” The handbook of Photonics, 2007.

[23] Rsoft’s BeamPROP Version 6.0 manual.

[24] Graham T. Reed, and Andrew P. Knights, “Silicon Photonics: An Introduction,” John Wiley & Sons, 2004.

[25] Tamir Theodor, “Guided-Wave Optoelectronics,” Springer-Verlag, 1990.

[26] Han, X.y., F.f. Pang, et al., "Characteristics of 980/1550 nm WDM coupler based on planar curved waveguides," Optik-International Journal for Light and Electron Optics **119**(2), 69-73 (2006).